ELECTROEXCITATION OF NUCLEON RESONANCES

VOLKER D. BURKERT
Jefferson Lab, 12000 Jefferson Avenue, Newport News, VA23606

Recent electroproduction results in the domain of s-channel nucleon resonance excitation are presented, and preliminary data in the search for missing states will be discussed. I also address a new avenue to pursue N^* physics using exclusive deeply virtual Compton scattering, recently measured for the first time at JLab and DESY.

1 Why N^*'s are important

Nucleon physics today is focussed on understanding the details of the nucleon spin and flavor structures at varying distances, and on the systematics of the baryon spectrum which reveals properties of the underlying symmetry structure.

Resonance electroproduction has rich applications in nucleon structure studies at intermediate and large distances. Resonances play an important role in understanding the spin structure of the nucleon [2,3]. More than 80% of the helicity-dependent integrated total photoabsorption cross section difference (GDH integral) is a result of the excitation of the $\Delta(1232)$ [4,2]. At $Q^2 = 1\text{GeV}^2$ about 40% of the first moment $\Gamma_1^P(Q^2) = \int_0^1 g_1(x,Q^2)dx$ for the proton is due to contributions of the resonance region at $W < 2\text{GeV}$ [5,6]. Conclusions regarding the nucleon spin structure for $Q^2 < 2\text{GeV}^2$ must therefore be regarded with some scepticism if contributions of baryon resonances are not taken into account.

The nucleon's excitation spectrum has been explored mostly with pion beams. Many states, predicted in the standard quark model, have not been seen in these studies, possibly many of them decouple from the $N\pi$ channel [7]. Electromagnetic interaction and measurement of multi-pion final states, may then be the only way to study some of these states. While photoproduction is one way [8], electroproduction, though harder to measure, adds additional sensitivity due to the possibility of varying the photon virtuality.

Electroexcitation in the past was not considered a tool of baryon spectroscopy. CLAS is the first full acceptance instrument with sufficient resolution to measure exclusive electroproduction of mesons with the goal of studying the excitation of nucleon resonances in detail. This feature is illustrated in Fig. 1, where the invariant mass W of the hadronic system is plotted versus the missing mass of the $ep \rightarrow epX$, where X represents the undetected

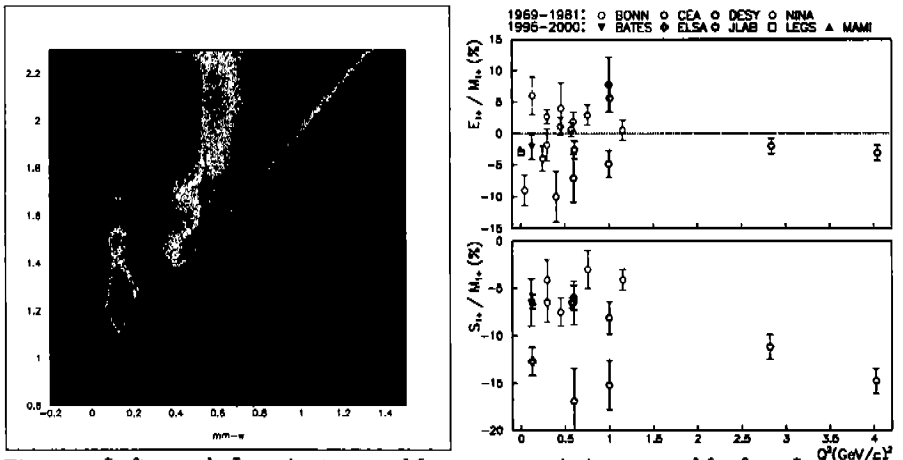

Figure 1. Left panel: Invariant mass $M_{\gamma^* p}$ versus missing mass M_X for $\gamma^* p \rightarrow pX$, measured in CLAS. Right panel: R_{EM} and R_{SM} before the year 2001.

system. The π^o, η, and ω bands are correlated with enhancements in the invariant mass, and indicate resonances coupling to $p\pi^o$ $p\eta$, and possibly $p\omega$ channels. Some of the lower mass states are already well known. However, their photocouplings and the Q^2 evolution of the transition form factors may be quite uncertain, or completely unknown.

2 Quadrupole Deformations of the Nucleon and Δ

An interesting aspects of nucleon structure at low energies is a possible quadrupole deformation of the nucleon. In the interpretation of ref. [9] this would be evident in non-zero values of the quadrupole transition amplitudes E_{1+} and S_{1+} from the nucleon to the $\Delta(1232)$. In models with $SU(6)$ spherical symmetry, this transition is due to a magnetic dipole M_{1+} mediated by a simple spin flip from the $J = \frac{1}{2}$ nucleon ground state to the Delta with $J = \frac{3}{2}$. Non-zero values for E_{1+} would indicate deformation. Dynamically such deformations may arise through interaction of the photon with the pion cloud [10,11] or through the one-gluon exchange mechanism [7]. At asymptotic momentum transfer, a model-independent prediction of helicity conservation requires $R_{EM} \equiv E_{1+}/M_{1+} \rightarrow +1$. An interpretation of R_{EM} in terms of a quadrupole deformation can therefore only be valid at low momentum transfer.

The data before 2001 (Fig. 1) show large systematic discrepancies. Taken together no clear trend is visible. At the photon point recent data from MAMI

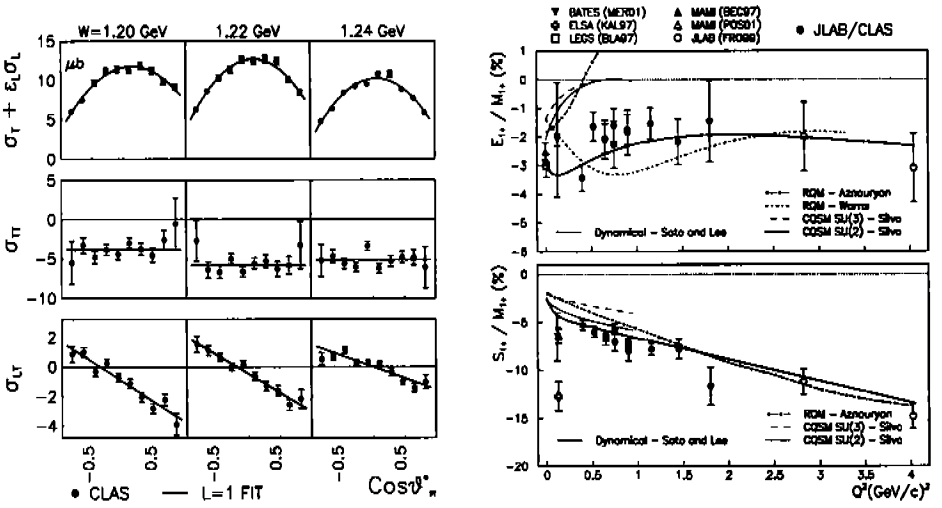

Figure 2. Left panel: Response functions for $p\pi^o$ in the Delta region measured with CLAS. Right panel: R_{EM} and R_{SM} after 1990, including the latest CLAS results covering the range Q^2=0.4 - 1.8GeV^2.

[12] and LEGS [13] are consistent with a value of $R_{EM} = -0.0275 \pm 0.005$.

The differential cross section for single pion production is given by

$$\frac{d\sigma}{d\Omega_\pi} = \sigma_T + \epsilon_L\sigma_L + \epsilon\sigma_{TT}\cos 2\phi + \sqrt{2\epsilon_L(\epsilon+1)}\sigma_{LT}\cos\phi + h\sqrt{\epsilon_L(1-\epsilon)}\sigma_{LT'}\sin\phi, \quad (1)$$

where ϕ is the azimuthal angle of the pion, and h=$\pm$1 is the helicity of the incident electron. The response functions σ_i depend on the hadronic invariant mass W, Q^2, and polar cms pion angle θ^*_π. CLAS allows measurement of the full angular distribution in azimuthal and in polar angle. The former allows separation of the ϕ-dependent and ϕ-independent response functions σ_i at fixed Q^2, W, and $\cos\theta^*_\pi$, while the latter contains information on the multipolarity of the transition. The multipoles can be extracted in some approximation through a fit of Legendre polynomials to the angular distribution of the various response functions. Angular distributions of response functions at fixed W values and results of the multipole analysis of the CLAS data [20] are shown in Fig. 2, where data from previous experiments published after 1990 are included as well [12,14]. R_{EM} remains negative and small throughout the Q^2 range. There are no indications that leading pQCD contributions are important as they would result in a rise of $R_{EM} \to +1$ [15]. R_{SM} behaves quite differently. While it also remains negative, its magnitude is strongly ris-

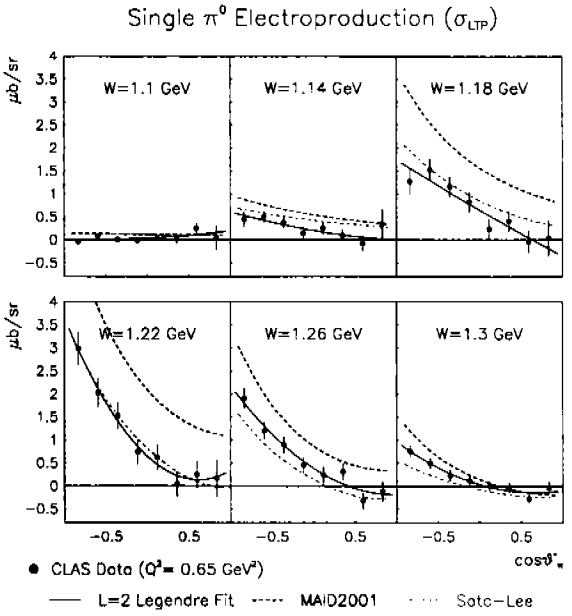

Figure 3. Preliminary $\sigma_{LT'}$ data from CLAS compared to two predictions of dynamical models. The data indicate strong model sensitivity.

ing with Q^2. For $Q^2 > 0.35\text{GeV}^2$ R_{SM} follows approximately a straight line that may be parametrized as: $R_{SM} = -(0.04 + 0.028 \times Q^2(\text{GeV}^2))$. The comparison with microscopic models, from relativized quark models [17,18], chiral quark soliton model [16], and dynamical models [10,11] show that simultaneous description of both R_{EM} and R_{SM} is achieved by dynamical models that include the nucleon pion cloud, explicitely. This supports the claim that most of the quadrupole strength is due to meson effects which are not included in other models.

Ultimately, we want to come to a QCD description of these important nucleon structure quantities. Currently, there is only one calculation in quenched QCD [19] giving $R_{EM} = 0.03 \pm 0.08$, which, due to the large uncertainty, has no bearing on our understanding of nucleon structure. This calculation was made nearly a decade ago. Improvements in computer performance and improved QCD actions and lattices should allow a reduction of the error to a level where QCD should provide significant input.

The new data establish a new level of accuracy. However, improvements in statistics and the coverage of a larger Q^2 range are expected for the near

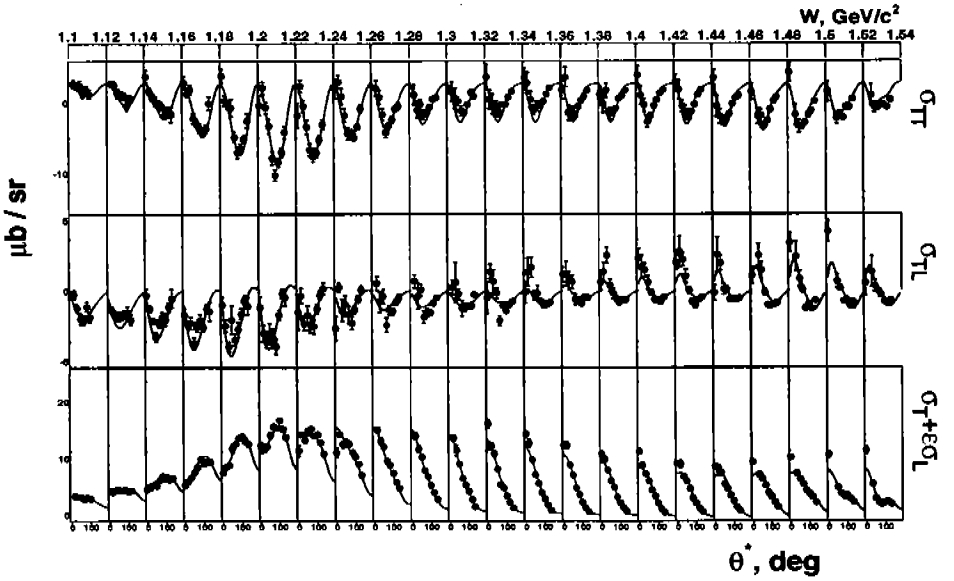

Figure 4. Response functions for $\gamma^* p \to n\pi^+$. The data cover the $\Delta(1232)$ and the 2nd resonance regions. Angular distributions are show for each bin in W. The data provide the basis for the analysis with a unitary isobar model (curve).

future, and they must be complemented by a reduction of model dependencies in the analysis. Model dependencies are largely due to our poor knowledge of the non-resonant terms, which become increasingly important at higher Q^2. The $\sigma_{LT'}$ response function, a longitudinal/transverse interferences term is especially sensitive to non-resonant contributions if a strong resonance is present. $\sigma_{LT'}$ can be measured using a polarized electron beam in out-of-plane kinematics for the pion. Preliminary data on $\sigma_{LT'}$ from CLAS are shown in Fig. 3 in comparison with dynamical models, clearly showing the model sensitivity to non-resonant contributions. Both models predict nearly the same unpolarized cross sections, however they differ in their handling of non-resonant contributions.

3 N^*'s in the Second Resonance Region

Three states, the elusive "Roper" $N'_{1/2^+}(1440)$, and two strong negative parity states, $N^*_{3/2^-}(1520)$, and $N^*_{1/2^-}(1535)$ make up the second enhancement seen in inclusive electron scattering. All of these states are of special interest to

obtain a better understanding of nucleon structure and strong QCD.

3.1 The Roper resonance - still a mystery

The Roper resonance has been a focus of attention for the last decade, largely due to the inability of the standard constituent quark model to describe basic features such as the mass, photocouplings, and their Q^2 evolution. This has led to alternate approaches where the state is assumed to have a strong gluonic component [21], a small quark core with a large meson cloud [22], or a hadronic molecule of a nucleon and a hypothetical *sigma* meson $|N\sigma>$ [23]. Lattice QCD calculations [25] show no sign of a 3-quark state with the quantum numbers of the nucleon in the mass range of the Roper state.

Experimentally, the Roper as a isospin 1/2 state couples more strongly to the $n\pi^+$ channel than to the $p\pi^o$ channel. Lack of data in that channel and lack of polarization data has hampered progress in the past. Fortunately, this sitation is changing significantly with the new data from CLAS. For the first time complete angular distributions have been measured for the $n\pi^+$ final state. Preliminary separated response functions obtained with CLAS are shown in Fig. 4. These data, together with the $p\pi^o$ response functions, as well as the spin polarized $\sigma_{LT'}$ response function for both channels have been fitted to a unitary isobar model. The results are shown in Fig. 5 together with the sparse data from previous analyses. None of the models gives a quantitaive description of the data. Much improved data are needed for more definite tests in a large Q^2 range. An interesting question is if the $A_{1/2}(Q^2)$ amplitude changes sign, or remains negative. The range of model predictions for the Q^2 evolution illustrates dramatically the sensitivity of electroproduction to the internal structure of this state.

3.2 The first negative parity state $N^*_{1/2^-}(1535)$

Another state of interest in the 2nd resonance region is the $N^*_{1/2^-}(1535)$. This state was found to have an unusually hard transition formfactor, i.e. the Q^2 evolution shows a slow fall-off. This state is often studied in the $p\eta$ channel which shows a strong s-wave resonance near the η-threshold with very little non-resonant background. Older data show some discrepancies as to the total width and photocoupling amplitude. In particular, analyses of pion photoproduction data[36] disagree with the analysis of the eta photoproduction data by a wide margin.

Data from CLAS[26], together with data from an earlier JLab experiment[27] give now a consistent picture of the Q^2 evolution, confirming the hard formfac-

tor behavior with much improved data quality, as shown in Fig. 6. Analysis of the $n\pi^+$ and $p\pi^o$ data at $Q^2 = 0.4 GeV^2$ gives a value for $A_{1/2}$ consistent with the analysis of the $p\eta$ data [24].

The hard transition formfactor has been difficult to understand in models. Recent work within a constituent quark model using a hypercentral potential [29] has made progress in reproducing the $A_{1/2}$ amplitude for the $N^*_{1/2^-}(1535)$, as well as for the $N^*_{3/2^-}(1520)$. The hard formfactor is also in contrast to models that interpret this state as a $|\bar{K}\Sigma>$ hadronic molecule [30]. Although no calculations exist from such models, the extreme "hardness" of the formfactor and the large cross section appear counter intuitive to an interpretation of this state as a bound hadronic system. Lattice QCD calculations also show very clear 3-quark strength for the state [7,25].

4 Higher Mass States and Missing Resonances

Approximate $SU(6) \otimes O(3)$ symmetry of the symmetric constituent quark model leads to relationships between the various states. In the single-quark transition model (SQTM) only one quark participates in the interaction. The model predicts transition amplitudes for a large number of states based on only a few measured amplitudes [31]. Comparison with photoproduction results show quite good agreement, while there are insufficient electroproduction data for a meaningfull comparison. The main reason is that many of the higher mass states decouple largely from the $N\pi$ channel, but couple dominantly to the $N\pi\pi$ channel. Study of $\gamma^* p \rightarrow p\pi^+\pi^-$ as well as the other charge channels are therefore important. Moreover, many of the so-called "missing" states are predicted to couple strongly to the $N\pi\pi$ channels [33].

4.1 A new resonances in the $p\pi^+\pi^-$ channel?

New CLAS total cross section electroproduction data are shown in Fig. 7 in comparison with photoproduction data from DESY [7]. The most striking feature is the strong resonance peak near W=1.72 GeV seen for the first time in electroproduction of the $p\pi + \pi-$ channel. This peak is absent in the photoproduction data. The CLAS data [32] also contain the complete hadronic angular distributions and $p\pi^+$ and $\pi^+\pi^-$ mass distributions over the full W range. They have been analyzed and the peak near 1.72GeV was found to be best described by a $N^*_{3/2^+}(1720)$ state. While there exists a state with such quantum numbers in this mass range, its hadronic properties were found previously to be very different from the CLAS state. For example, the PDG gives for the known state a $N\rho$ coupling of $\Gamma_{N\rho}/\Gamma_{tot}(PDG) \approx 0.85$ while the

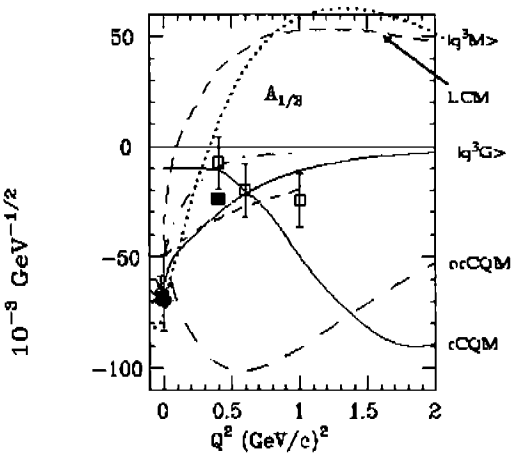

Figure 5. Transverse helicity amplitude $A_{1/2}(Q^2)$ for the Roper resonance. The full squared red symbol is a preliminary point from CLAS (see text). Comparisons with varies models are shown

CLAS state has a very small coupling to that channel $\Gamma_{N\rho}/\Gamma_{tot}(CLAS) \approx 0.17$. Also, other parameters such as the total width $\Gamma_{tot} = 88 \pm 17$MeV, and $\Gamma_{\Delta\pi}/\Gamma_{tot} = 0.41 \pm 0.13$, and the photocoupling amplitudes, are quite different from what is known or expected from the PDG state. The question arises if the state could be one of the "missing" states. Capstick and Roberts [33] predict a state with these quantum numbers at a mass 1.85GeV. There are also predictions of a hybrid baryon state with these quantum numbers at about the same mass [35], although the rather hard form factor disfavors the hybrid baryon interpretation [21]. As mass predictions in these models are uncertain to at least ±100MeV, interpretation of this state as a "missing" $N^*_{3/2^+}$ is a definite possibility. Independent of possible interpretations, the hadronic properties of the state seen in the CLAS data appear incompatible with the properties of the known state with same quantum numbers as listed in Review of Particle Properties [36].

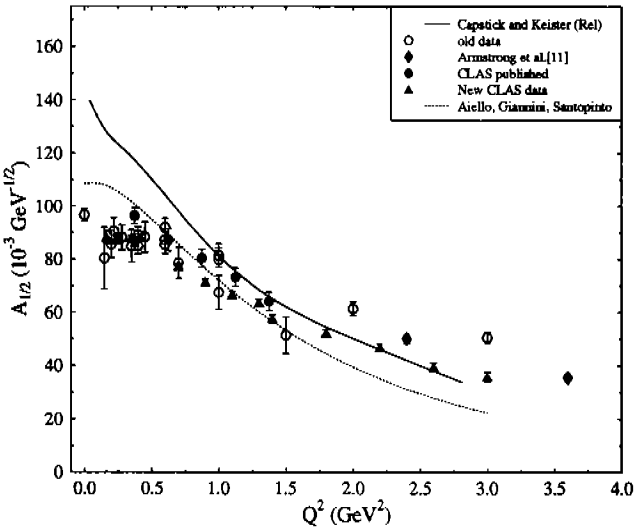

Figure 6. Transverse helicity amplitude $A_{1/2}(Q^2)$ for the first negative parity state $N^*_{1/2^-}(1535)$.

4.2 Hard nucleon spectroscopy

The analysis of the $p\pi^+\pi^-$ data within the Genova/Moscow isobar model[34] shows that the cross section ratio R= resonance/background at W = 1.7 GeV is strongly rising with Q^2, from R=0.3 at the photon point to R=1.8 at Q^2=1.3GeV^2. Therefore, electron scattering at relatively high photon virtuality, Q^2, can provide much increased sensitivity in the study of at least some of the higher mass resonances. Qualitatively, this can be understood within a non-relativistic dynamical quark model [37,7]. Photocoupling amplitudes for these states usually contain polynomials proportional to powers of the photon 3-momentum vector $|\vec{q}|$. For virtual photons the 3-momentum $|\vec{q}|$ for the transition to a given resonances increases with Q^2 leading to an enhancement. In the case of the $N^*_{3/2^+}$ the non-relativistic quark model predicts $A_{1/2} = C(|\vec{q}| + |\vec{q}|^3/3\alpha^2)F(|\vec{q}|)$, where α is the harmonic oscillator constant of the model, and $F(|\vec{q}|)$ a formfactor which is common to all states.

To the degree that non-relativistic kinematics can be applied, spectroscopy of higher mass states at higher photon virtualities ("hard spectroscopy") has a distinct advantage over the real photon case: as the power n in $|\vec{q}|^n$ depends on the specific $SU(6) \otimes O(3)$ multiplet a state is associated with, it allows enhancing the excitation of certain states over others by selecting specific Q^2 ranges.

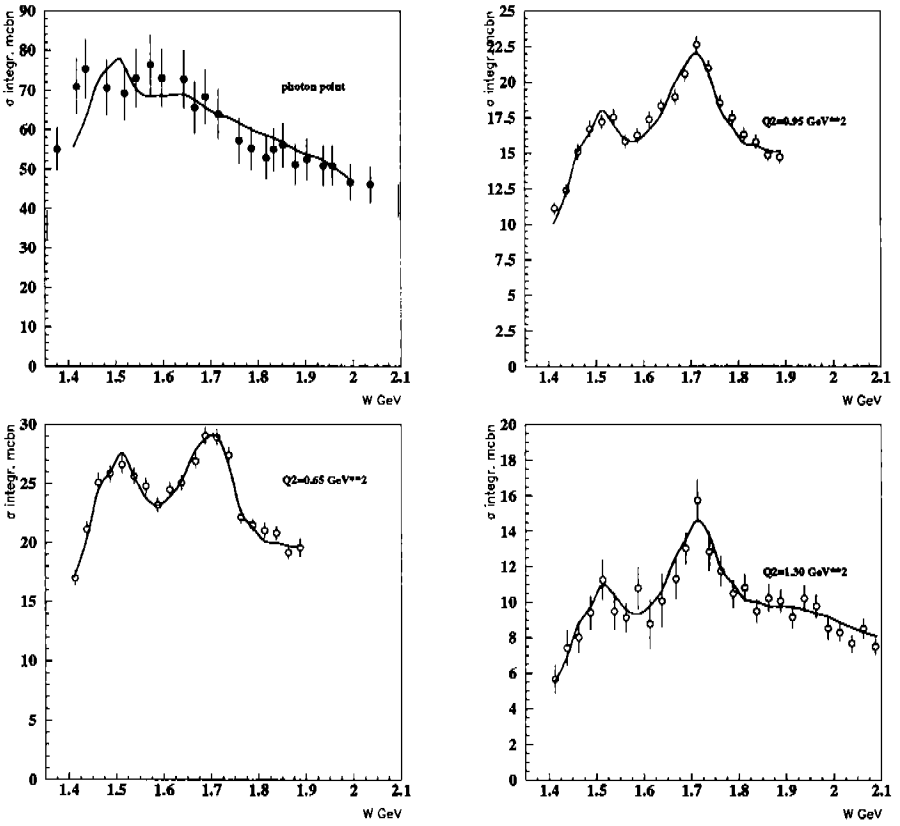

Figure 7. Total photoabsorption cross section for $\gamma^* p \rightarrow p\pi^+\pi^-$. Photoproduction data from DESY - top left panel. The other panels shows CLAS electroproduction data at $Q^2 = 0.65,\ 0.95, 1.30 GeV^2$.

4.3 Nucleon states in $K\Lambda$ production

Strangeness channels have recently been examined in photoproduction as a possible source of information on new baryon states, and candidate states have been discussed [28,8]. New CLAS electroproduction data [38] in the $K\Lambda$ channel show clear evidence for resonance excitations at masses of 1.7 and 1.85 GeV as show in Fig. 8. The analysis of the $K\Lambda$ channel is somewhat complicated by the large t-channel exchange contribution producing a peak at forward angles. To increase sensitivity to s-channel processes the data

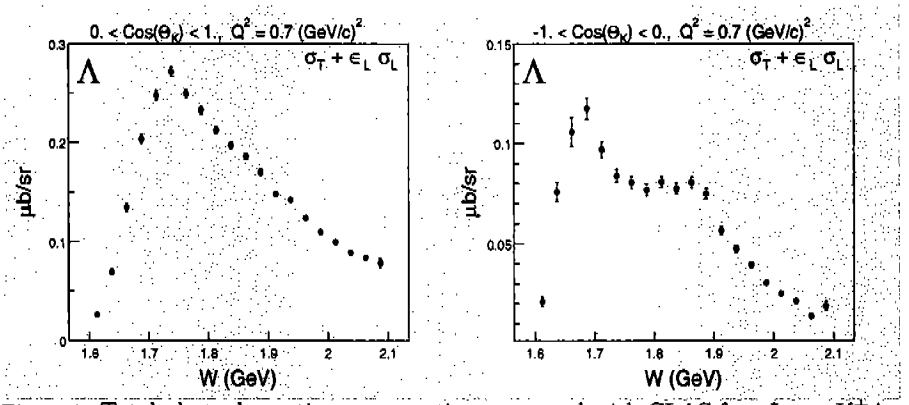

Figure 8. Total photoabsorption cross section measured with CLAS for $\gamma^* p \to K^+\Lambda$. The left panel is integrated over the full forward hemisphere in the K^+ angular distribution in the $K^+\Lambda$ cms. The right panel is integrated over the backward hemisphere

have been divided into a set for the forward hemisphere and for the backward hemisphere. Clear structures in the invariant mass emerge for the backward hemisphere (right panel in Fig. 8). While the lower mass peak is probably due to known resonances, the peak near 1.85GeV maybe associated with the bump observed with the SAPHIR detector [28]. A more complete analysis of the angular distribution and the energy-dependence is needed for more definite conclusions.

4.4 Resonances in Virtual Compton Scattering

Virtual Compton scattering, i.e. the process $\gamma^* p \to p\gamma$ is yet another tool in the study of excited baryon states. This process has recently been measured by experiment E93-050 in JLab Hall A [39] at backward photon angles. The excitation spectrum exhibits clear resonance excitations in the mass regions of known states, the $\Delta(1232)$, $N^*(1520)$, and $N^*(1650)$. The main advantage of this purely electromagnetic process is the absence of final state interaction. This interaction complicates the interpretation of hadronic channels. A disadvantage is the low rate that makes it difficult to collect sufficient statistics for a full partial wave analysis.

5 Baryon spectroscopy at short distances

Inelastic virtual Compton scattering in the deep inelastic regime (DVSC) can provide a new avenue of resonance studies at the elementary quark level. The process of interest is $\gamma^* p \to \gamma N^*(\Delta^*)$ where the virtual photon has a high virtuality (Q^2). The virtual photons couples to an elementary quark with longitudinal momentum fraction x, which is re-absorbed into the baryonic system with momentum fraction $x - \xi$, after having emitted a high energy photon. The recoil baryon system may be a ground state proton or an excited state. The elastic DVCS process has recently been measured at JLab [41] and at DESY [40] in polarized electron proton scattering, and the results are consistent with predictions from perturbative QCD and the twist expansion for the process computed at the quark-gluon level. The theory is under control for small momentum transfer to the final state baryon. For the inelastic process, where a N^* or Δ resonance is excited, the process can be used to study resonance transitions at the elementary quark level. Varying parameter ξ and the momentum transfer to the recoil baryon probes the two-parton correlation functions or generalized parton distributions (GPDs).

That this process is indeed present at a measureable level is seen in the preliminary data from CLAS [42] shown in in Fig. 9. The reaction is measured at invariant masses $W > 2$ GeV. The recoiling baryonic system clearly shows the excitation of resonances, the $\Delta(1232)$, $N^*(1520)$, and $N^*(1680)$. While these are well known states that are also excited in the usual s-channel processes, the DVCS process has the advantage that it decouples the photon virtuality Q^2 from the 4-momentum transfer to the baryon system. Q^2 may be chosen sufficiently high such that the virtual photon couples to an elementary quark, while the momentum transfer to the nucleon system can be varied independently from small to large values. In this way, a theoretical framework employing perturbative methods can be used to probe the "soft" NN^* transition, allowing to map out internal parton correlations for this transition.

6 Conclusions

Electroexcitation of nucleon resonances has evolved to an effective tool in studying nucleon structure in the regime of strong QCD and confinement. The new data from JLab in the $\Delta_{3/2^+}(1232)$ and $N^*_{1/2^-}(1535)$ regions give a consistent picture of the Q^2 evolution of the transition form factors. Large data sets in different channels including polarization observables will vastly improve the analysis of states such as the "Roper" $N'_{1/2^+}(1440)$, and many other higher mass states. A strong resonance signal near 1.72 GeV, seen

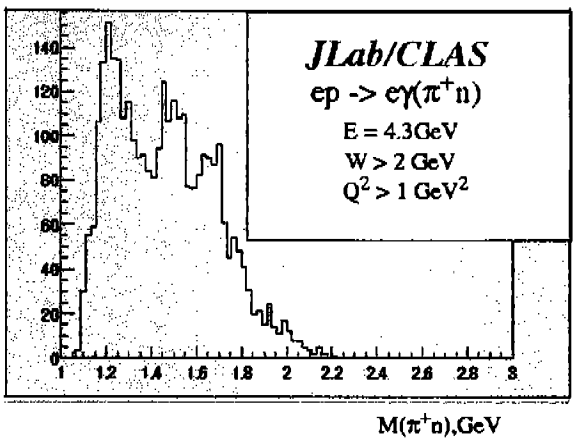

Figure 9. Inelastic deeply virtual Compton scattering measured in CLAS. The recoiling $(n\pi^+)$ system clearly shows the excitation of several resonances, the $\Delta(1232)$, $N^*(1520)$, and $N^*(1680)$.

with CLAS in the $p\pi^+\pi^-$ channel, exhibits hadronic properties which are incompatible with any of the known states in this mass region. While s-channel resonance excitation will remain the backbone of the N^* program for years to come, inelastic deeply virtual Compton scattering is a promising tool in resonance physics at the elementary parton level, which allows the study of parton-parton correlations within a well defined theoretical framework.

The Southeastern Universities Research Association (SURA) operates the the Thomas Jefferson National Accelerator Facility for the United States Department of Energy under Contract No. DE-AC05-84ER40150.

References

1. N. Isgur, in: Excited Nucleons and Hadron Structure, World Scientific, 2001, eds.: V. Burkert, L. Elouadrhiri, J. Kelly, R. Minehart.
2. V.D. Burkert, and Zh. Li, Phys.Rev.D47:46-50,1993
3. V.D. Burkert and B.L. Ioffe, Phys.Lett.B296:223-226,1992; J.Exp.Theor.Phys.78:619-622,1994
4. J. Ahrens et al., Phys.Rev.Lett.87:022003,2001
5. R. De Vita, this conferences
6. V.D. Burkert, Nucl.Phys.A699:261-269,2002
7. R. Koniuk and N. Isgur, Phys.Rev.D21:1868,1980
8. A. d'Angelo, this conference

9. A. Buchmann and E. Henley, Phys.Rev.D65:073017,2002
10. T. Sato and T.S. Lee, T. Sato, this conferences
11. S.S. Kamalov and S.N. Yang, Phys.Rev.Lett.83:4494-4497,1999
12. R. Beck et al., Phys.Rev.C61:035204,2000
13. G. Blanpied et al., Phys.Rev.C64:025203,2001
14. V.V. Frolov et al., Phys.Rev.Lett.82:45-48,1999
15. G. A. Warren, C.E. Carlson, Phys.Rev.D42:3020-3024,1990
16. A. Silva et al., Nucl.Phys.A675:637-657,2000
17. M. Warns, H. Schroder, W. Pfeil, H. Rollnik, Z.Phys.C45:627,1990
18. I.G. Aznaurian, Z.Phys.A346:297-305,1993
19. D. Leinweber, T. Draper, R.M. Woloshyn, Phys.Rev.D48:2230-2249,1993
20. K. Joo, et al, Phys. Rev. Lett. 88, 122001,2002; L.C. Smith, this conferences
21. Z.P. Li, V. Burkert, Zh. Li; Phys.Rev.D46, 70, 1992
22. F. Cano and P. Gonzales, Phys.Lett.B431:270-276,1998
23. O. Krehl, C. Hanhart, S. Krewald, J. Speth, Phys.Rev.C62:025207,2000
24. H. Egiyan, this conference
25. S. Sasaki, T. Blum, S. Ohta Phys.Rev.D65:074503
26. R. Thompson et al., Phys.Rev.Lett.86, 1702 (2001), H. Denizli, this conference
27. C.S. Armstrong et al., Phys.Rev.D60:052004,1999
28. M.Q. Tran et al., Phys.Lett.B445:20-26,1998
29. M.M. Giannini, E. Santopinto, A. Vassallo, Nucl.Phys.A699:308-311,2002; E. Santopinto, this conference
30. N. Kaiser, P.B. Siegel, W. Weise, Phys.Lett.B362:23-28,1995
31. W.N. Cottingham and I.H. Dunbar, Z.Phys.C2, 41, 1979
32. M. Ripani, Nucl.Phys.A699:270-277,2002
33. S. Capstick and W. Roberts, Phys.Rev.D49:4570-4586,1994
34. V.I. Mokeev, et al., Phys.Atom.Nucl.64:1292-1298,2001
35. S. Capstick, P.R. Page, Phys.Rev.D60:111501,1999
36. D.E. Groom et al., Eur.Phys.J. C15, 1-878, 2000
37. L.A. Copley, G. Karl, E. Obryk, Nucl.Phys.B13:303-319,1969
38. G. Niculescu, this conferences; R. Feuerbach, private communications.
39. H. Fonvieille, this conferences
40. A. Airapetian et al., Phys.Rev.Lett.87, 182001-1(2001)
41. S. Stepanyan et al., Phys.Rev.Lett.87,182002-1(2001)
42. M. Guidal, private communications (2002)